Supplementary Information for:

Disentangling the sequence, cellular and ultrastructural determinants of Huntingtin nuclear and cytoplasmic inclusion formation.

Nathan Riguet[1], Anne-Laure Mahul-Mellier[1], Niran Maharjan[1], Johannes Burtscher[1], Alice Patin[1], Marie Croisier[2], Graham Knott[2], Veronika Reiterer[3], Hesso Farhan[3] and Hilal A. Lashuel[1]*

*Correspondence: hilal.lashuel@epfl.ch

Affiliations:

[1]Laboratory of Molecular and Chemical Biology of Neurodegeneration, Brain Mind Institute, Ecole Polytechnique Fédérale de Lausanne (EPFL), 1015 Lausanne, Switzerland.

[2]BIO EM facility (BIOEM), EPFL, 1015 Lausanne, Switzerland.

[3]Institute of Basic Medical Sciences, University of Oslo, Norway.

This document file includes:

Figures

A

Primary Antibody	Reference	Company	Clone	RRID	Host	ICC Dilution	WB Dilution	Epitope
Anti Htt	2B7	CHDI	2b7	-	Mouse monoclonal	1/500	-	Nt17 domain
Anti Htt	Ab109115	Abcam	EPR5526	AB_10863082	Rabbit polyclonal	1/500	-	Nt17 domain
Anti Htt	MW1	CHDI	MW1	AB_528290	Mouse	1/500	-	PolyQ
Anti Htt	MAB5492	Millipore	2B4	AB_11213848	Mouse monoclonal	1/500	1/5000	50–64
Anti Htt	4C9	CHDI	4C9	-	Mouse	1/500	-	PRD domain
Anti Htt	N18 (sc-8767)	Santa-Cruz	3E10	AB_2123254	goat polyclonal	1/500	-	aa 50-100
Anti Htt	MW8	CHDI	MW8	AB_528297	Mouse monoclonal	1/500	-	C-ter (mHtt)
Anti Htt	S830	Bates lab	-	-	Sheep	1/500	-	mHttex1
Anti Htt	Eurogentec (414-4D3G9A12)	Lashuel lab	-	-	Mouse monoclonal	1/500	-	Httex1
Anti Bera-actin	ab6276	Abcam	AC-15	AB_2223210	Mouse	-	1/5000	DDDIAALVIDNGSGK
Anti BIP/Grp78	ab21685	Abcam	-	AB_2119834	Rabbit	1/500	-	-
Anti Tom20	sc-17764	Santa-Cruz	F-10	AB_628381	Mouse	1/500	-	Raised against amino acids 1-145
Anti p62	H00008878	Abnova	2C11	AB_437085	Mouse	1/500	-	Raised against a full length recombinant SQSTM1
Anti Vimentin	ab92547	Abcam	EPR3776	AB_10562134	Rabbit	1/500	-	Synthetic peptide within Human Vimentin aa 400 to the C-terminus
Anti HDAC6	ab1440	Abcam	-	AB_2232905	Rabbit	1/500	-	Synthetic peptide (Mouse) - N terminal
Anti Sec13	MAB9055	R&D Systems	1280A	-	Rabbit monoclonal	1/500	-	
Anti VDAC1	ab14734	Abcam	20B12AF2	AB_443084	Mouse	-	1/5000	Recombinant full length protein corresponding to Human VDAC1/ Porin.

B

Secondary Antibody	Reference	Company	RRID	ICC Dilution	WB Dilution
Donkey anti-rabbit Alexa Fluor 647	A31573	Invitrogen	RRID:AB_2536183	1/800	
Donkey anti-mouse Alexa Fluor 647	A31571	Invitrogen	RRID:AB_162542	1/800	
Goat anti-mouse Alexa Fluor 680	A21058	Invitrogen	RRID:AB_2535724		1/5000
Goat anti-rabbit Alexa Fluor 680	A21109	Invitrogen	RRID:AB_2535758		1/5000
Goat anti-mouse Alexa Fluor 800	926-32210	Li-Cor	RRID:AB_621842		1/5000
Goat anti-rabbit Alexa Fluor 800	926-32211	Li-Cor	RRID:AB_621843		1/5000

Figure S1. List of the antibodies used in this study.

A. Primary antibodies used in this study. **B.** Secondary antibodies used in this study.

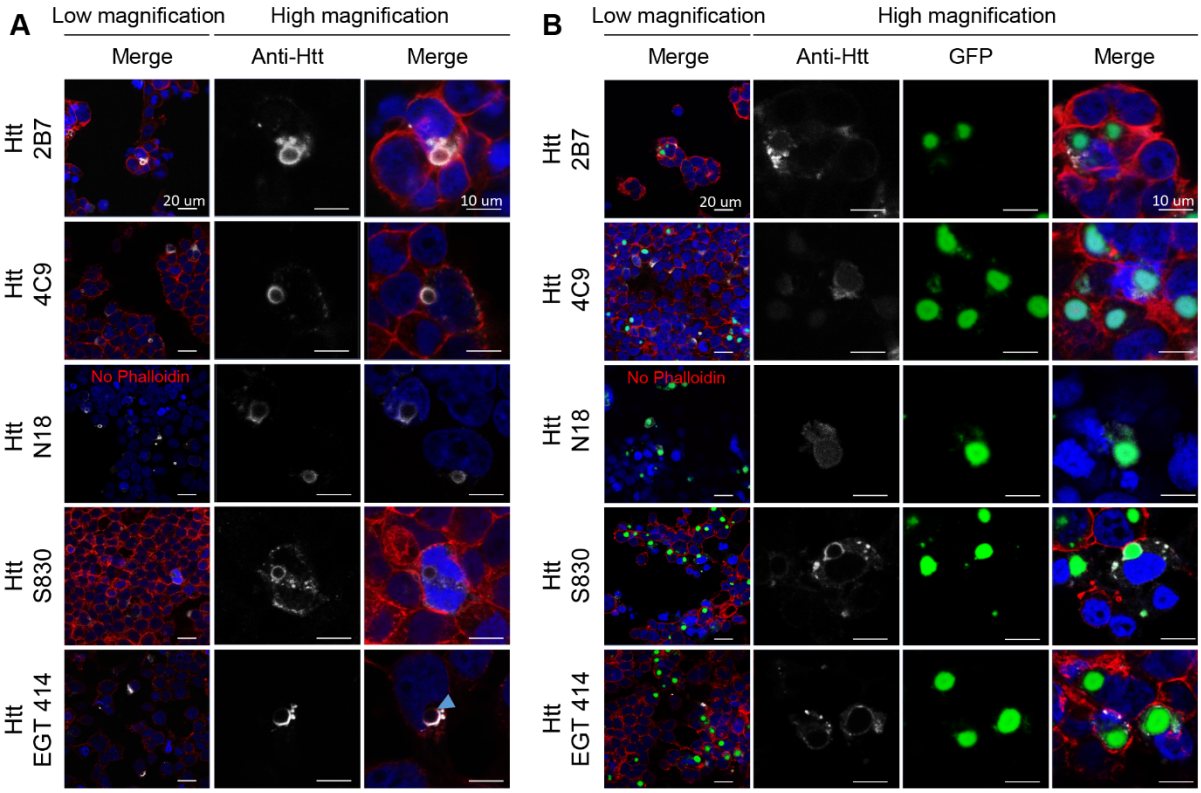

Figure S2. Characterization of Httex1 72Q and Httex1 72Q-GFP inclusions by Immunocytochemistry with a panel of Httex1 antibodies revealed a ring-like detection. **A.** ICC of HEK cells transfected with Httex1 72Q-GFP for 48h. (**A-B**) Httex1 72Q and Httex1 72Q-GFP inclusions were detected as a ring-like structure with all the Htt antibodies tested (grey) and as puncta with the GFP channel (green). Blue arrows indicate F-actin (red) colocalizing with the ring-like structure of some Httex1 72Q inclusion. DAPI was used to counterstain the nucleus. Scale bar = 20 µm (left-hand panels) and 10 µm (middle and right-hand panels).

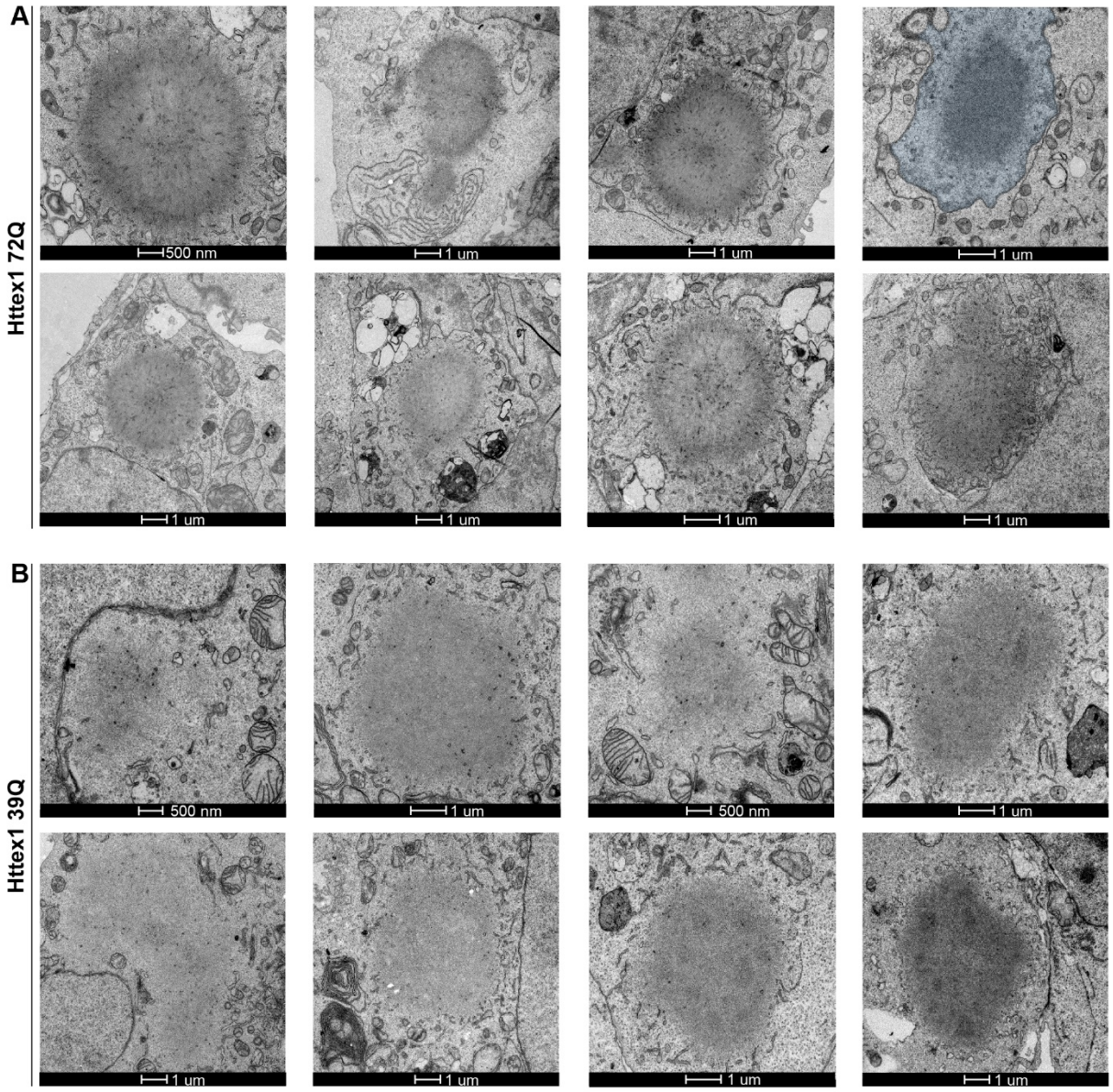

Figure S3. Ultrastructural characterization of Httex1 72Q and Httex1 39Q inclusions. A. 8 representative electron micrographs of Httex1 72Q inclusions in HEK cells 48h post-transfection. **B.** 8 representative electron micrographs of Httex1 39 inclusions in HEK cells 48h post-transfection. The nucleus was highlighted in blue. Scale bar = 1 μm or 500 nm as indicated below the micrographs.

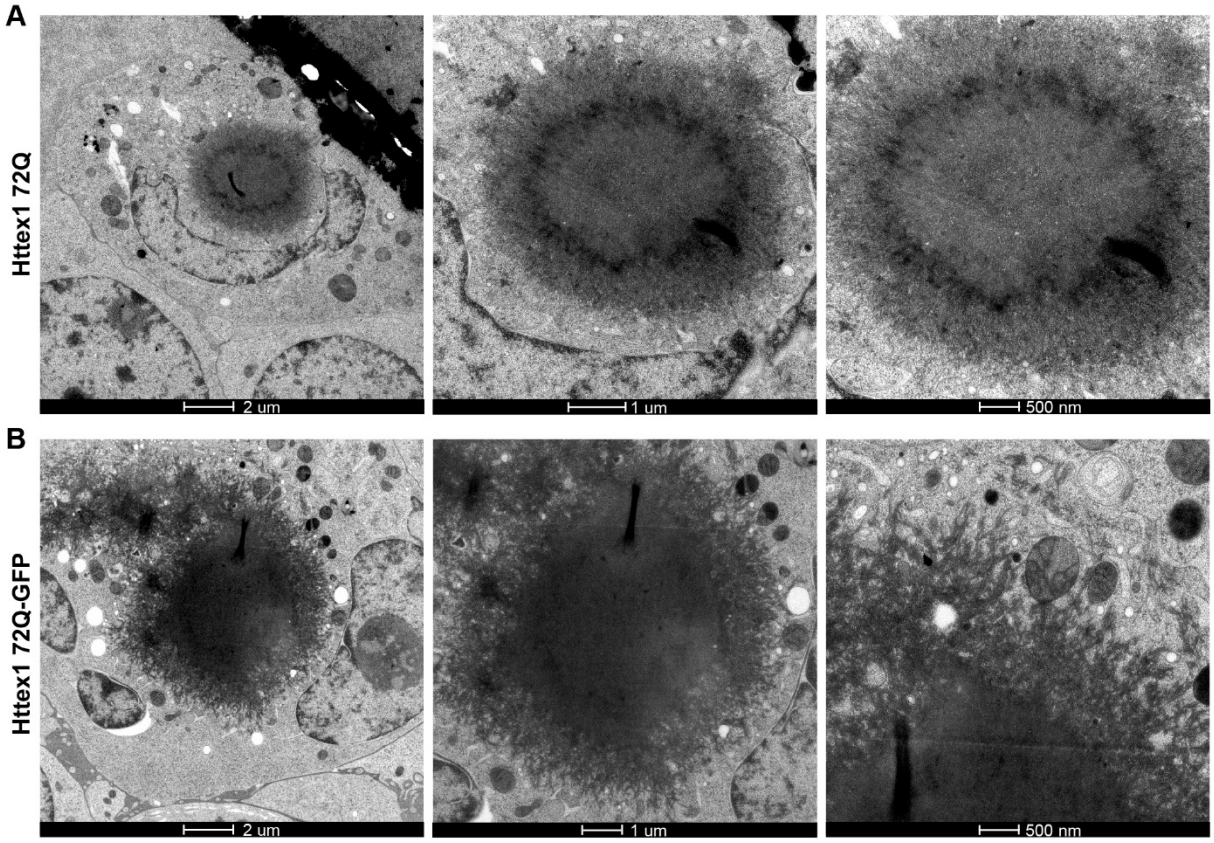

Figure S4. Electron microscopy analysis of Httex1 72Q and Httex1 72Q-GFP cellular inclusions post-High-Pressure Freezing (HPF) demonstrates a distinct fibrillar organization. HEK cells were fixed by HPF and freeze substituted for EM imaging 48h after Httex1 transfection. **A.** Electron micrographs of Httex1 72Q inclusion show radiating stacked fibrils. **B.** Electron micrographs of Httex1 72Q-GFP inclusion reveal think radiating fibrils at the periphery. Scale bar = 2 µm, 1 µm, or 500 nm as indicated below the micrographs.

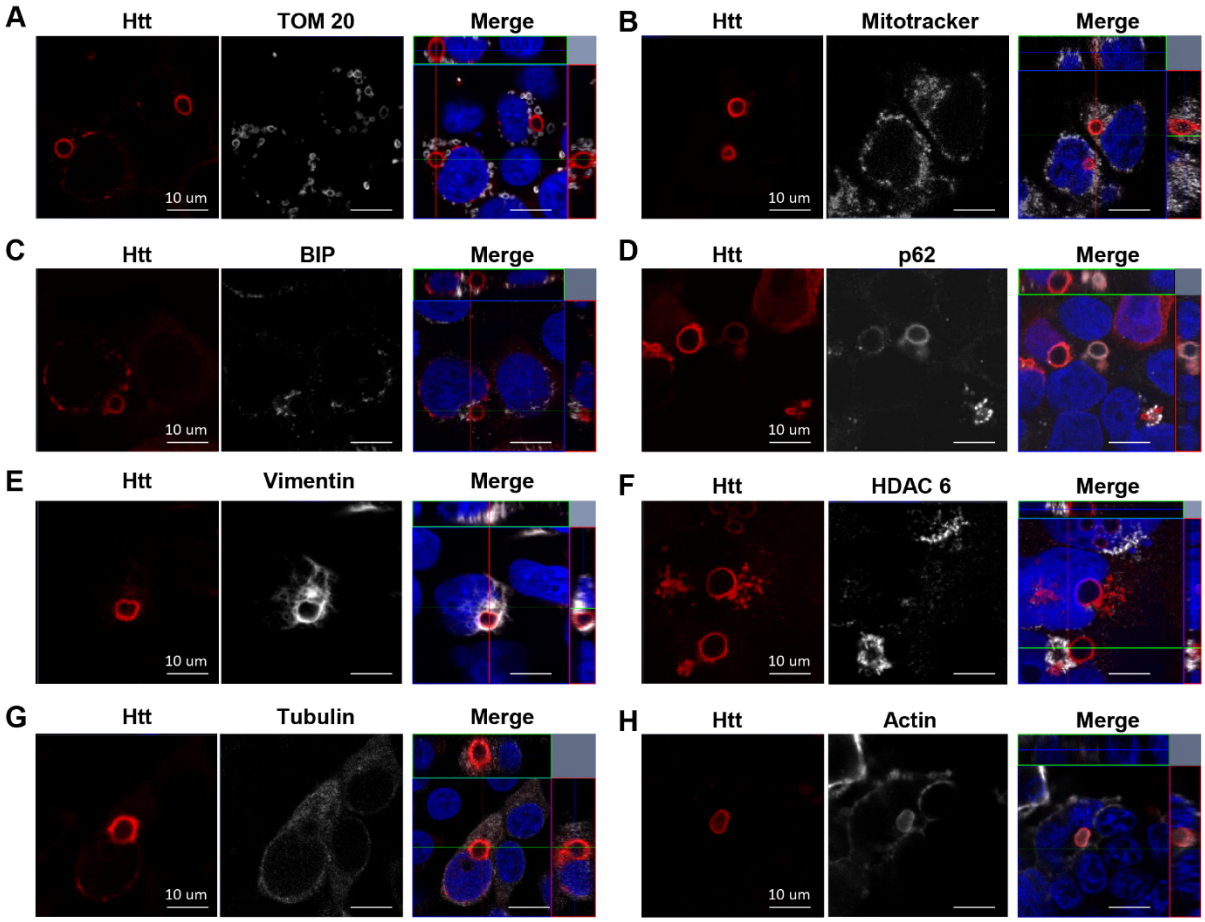

Figure S5. Formation of the Httex1 72Q cellular inclusions is accompanied by the accumulation of organelles at their periphery. Httex1 72Q inclusions formed in HEK cells 48h post-transfection were stained by Htt antibody (MAB5492, grey) in combination with organelle markers Tom20 and Mitotracker (mitochondria) (**A**), BIP (ER) (**C**), p62 (autophagosomes) (**D**), Vimentin (**E**) and HDAC6 (**F**) (aggresome), tubulin (**G**) and actin (**H**) (cytoskeleton). The nucleus was counterstained with DAPI (blue). Scale bars = 10 μm.

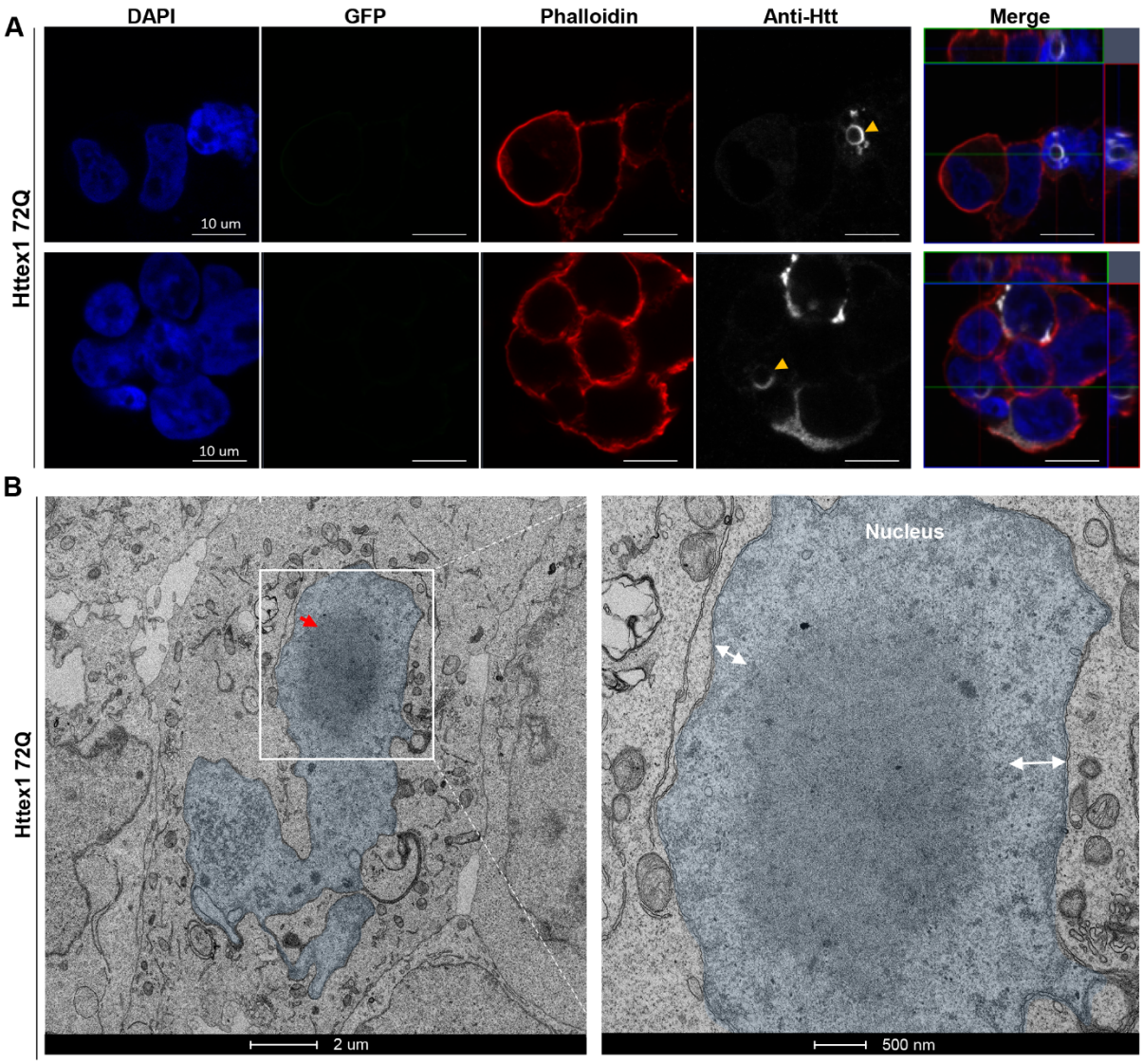

Figure S6. The nuclear inclusions formed by Httex1 72Q do not exhibit the classical core and shell organization observed for the cytosolic inclusions. A. Representative confocal images of Httex1 72Q nuclear inclusions, 48h after transfection. Httex1 expression (grey) was detected using a specific primary antibody against the N-terminal part of Htt (amino acids 1-17; 2B7 or Ab109115). The nucleus was counterstained with DAPI (blue), and phalloidin (red) was used to stain the actin F. Httex1 nuclear inclusions are indicated by the yellow arrowheads. Scale bars = 10 µm. **B.** Electron micrograph of a representative nuclear Httex1 72Q inclusion. The white square indicates the area shown at higher magnification in the right-hand panel. The nucleus is highlighted in blue and the double arrows indicate the distance between the nuclear inclusion and the nuclear membrane. No interaction between the nuclear inclusion and the nuclear membrane was observed. Scale bar = 2 µm (left-hand panel) and 500 nm (right-hand panel).

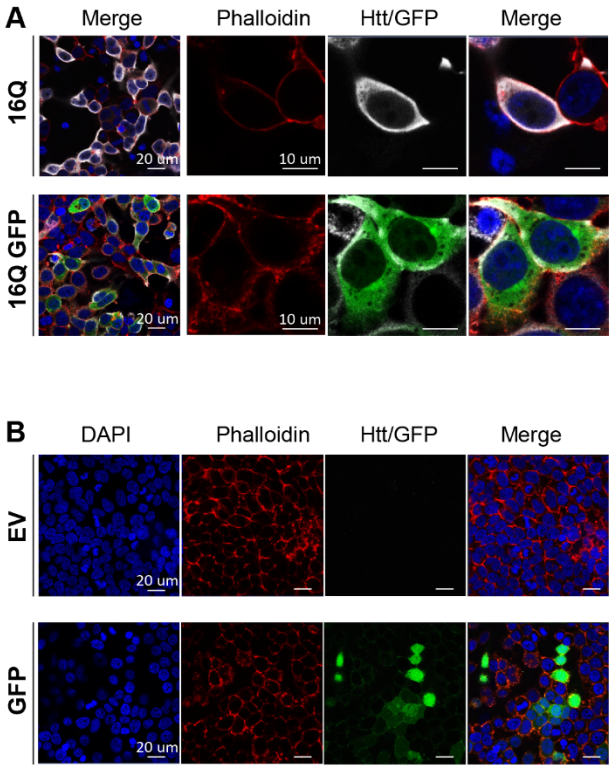

Figure S7. Immunocytochemistry of HEK cells expressing Httex1 16Q (+/-GFP) and EV/GFP controls does not show any aggregate formation. A. Representative confocal images of Httex1 16Q and Httex1 16Q-GFP do not display any aggregates 48h after transfection. Scale bar = 20 µm (left-hand panels) and 10 µm (middle right-hand panels). **B.** Representative confocal images of EV and GFP do not display any aggregates or Htt staining 48h after transfection. Scale bars = 20 µm.

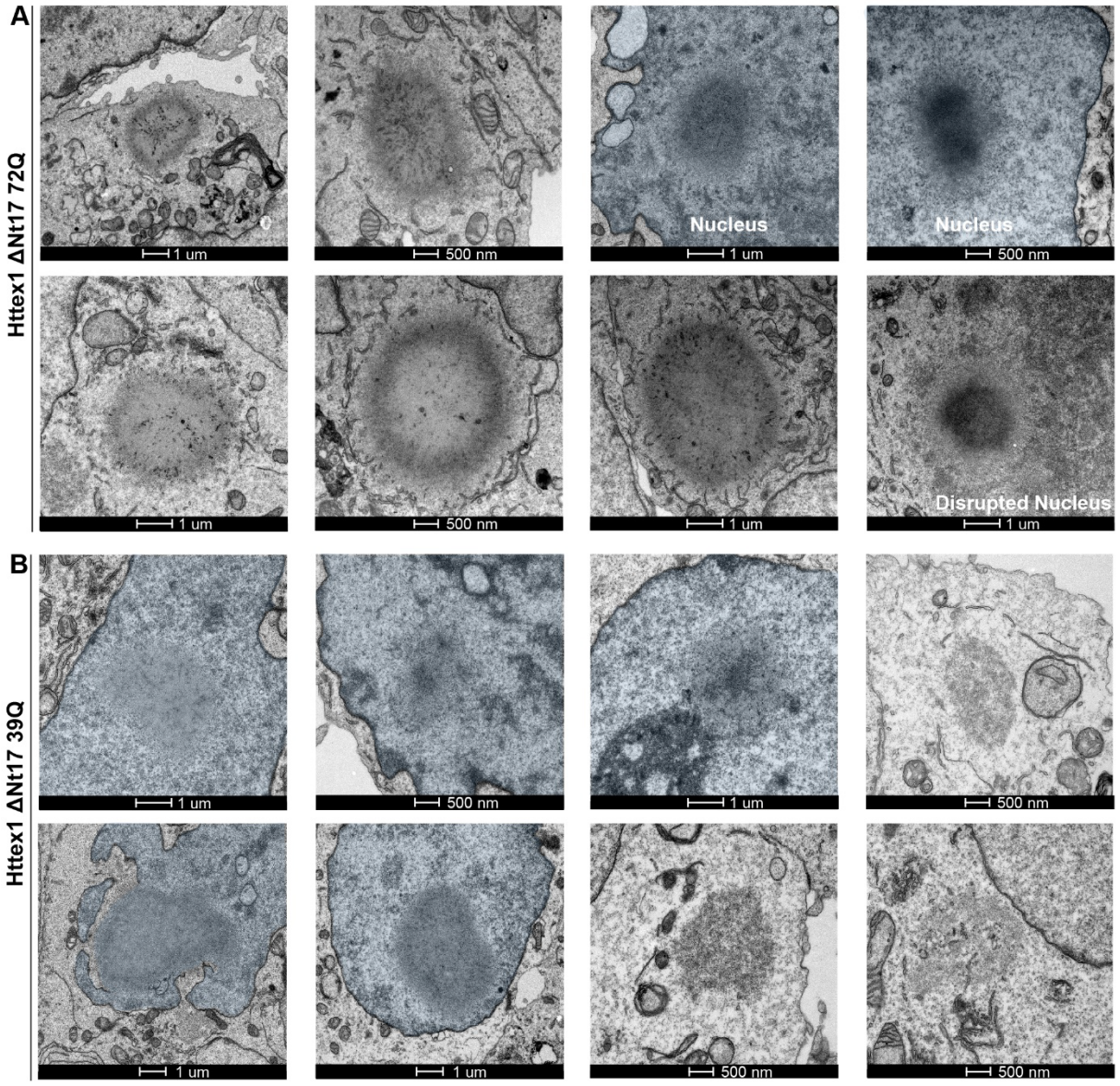

Figure S8. Ultrastructural characterization of Httex1 ΔNt17 72Q and Httex1 ΔNt17 39Q inclusions. A. 8 representative electron micrographs of Httex1 ΔNt17 72Q inclusions in HEK cells 48h post-transfection. **B.** 8 representative electron micrographs of Httex1 ΔNt17 39 inclusions in HEK cells 48h post-transfection. The nucleus is highlighted in blue. Scale bar = 1 µm or 500 nm as indicated below the micrographs.

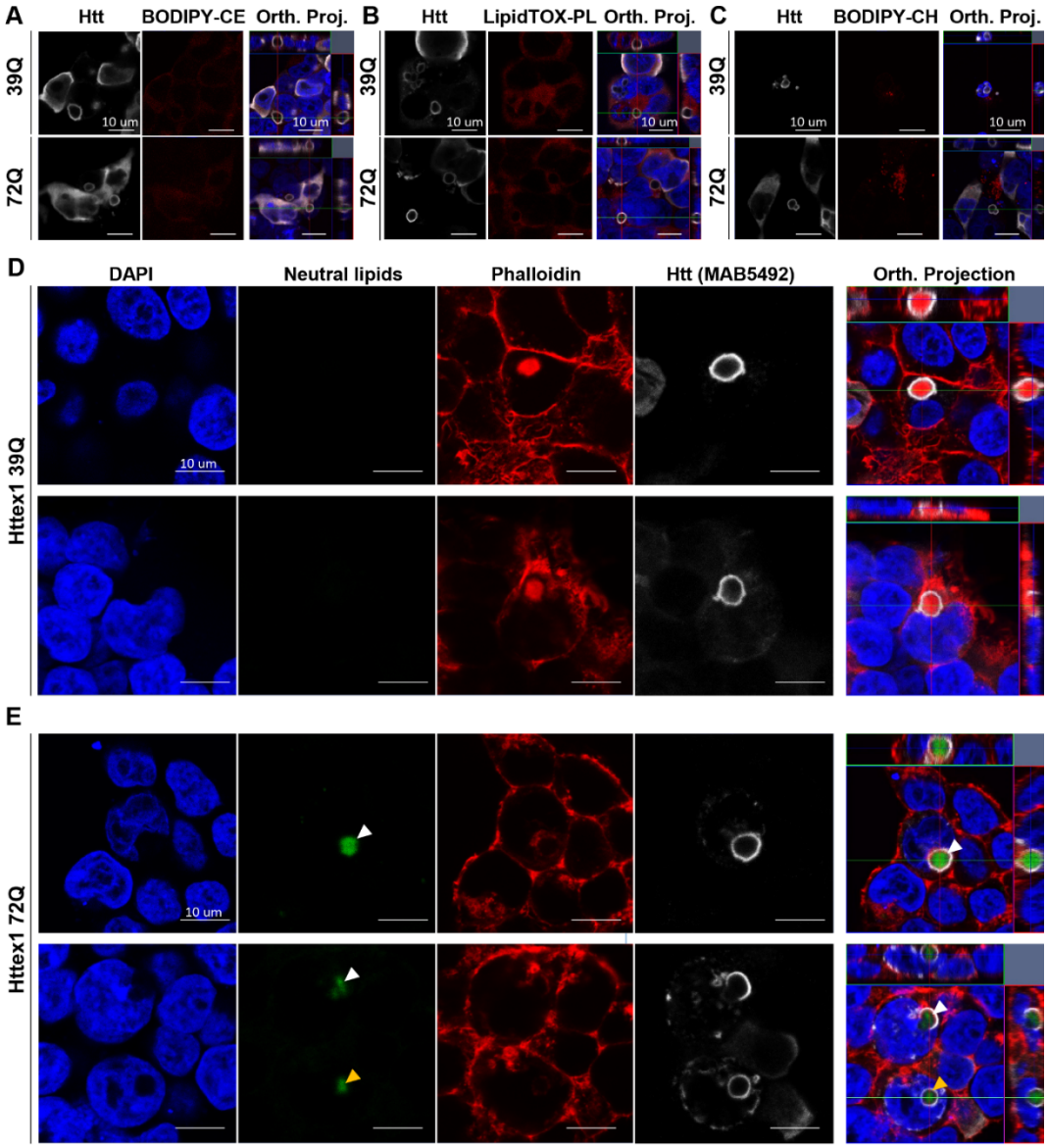

Figure S9. Neutral lipid enrichment of Httex1 cellular inclusions is dependent on the polyQ length. (A-C) Representative confocal images of Httex1 39Q and Httex1 72Q inclusions 48h post-transfection stained by Htt antibody (MAB5492, grey) and different lipid dyes (red). **A.** The Ceramide BODIPY probe (BODIPY-CE) does not show any colocalization of inclusions with Ceramide. **B.** The LipidTOX™ Red phospholipid stain (LipidTOX-PL) does not show any colocalization of inclusions with phospholipids. **C.** The cholesteryl ester BODIPY probe (BODIPY-CH) does not show any colocalization of inclusions with cholesteryl ester. Scale bars = 10 µm. Representative confocal images of Httex1 39Q **(D)** and Httex1 72Q **(E)** inclusions formed 48h after transfection in HEK cells. Inclusions were stained by the Htt antibody (MAB5492, grey) in combination with a marker of the neutral lipids (non-Polar BODIPY probe, green). The nucleus was counterstained with DAPI (blue), and phalloidin (red) was used to stain the actin F. White arrowheads indicate neutral lipid enrichment only for Httex1 72Q inclusions. Scale bars = 10 µm.

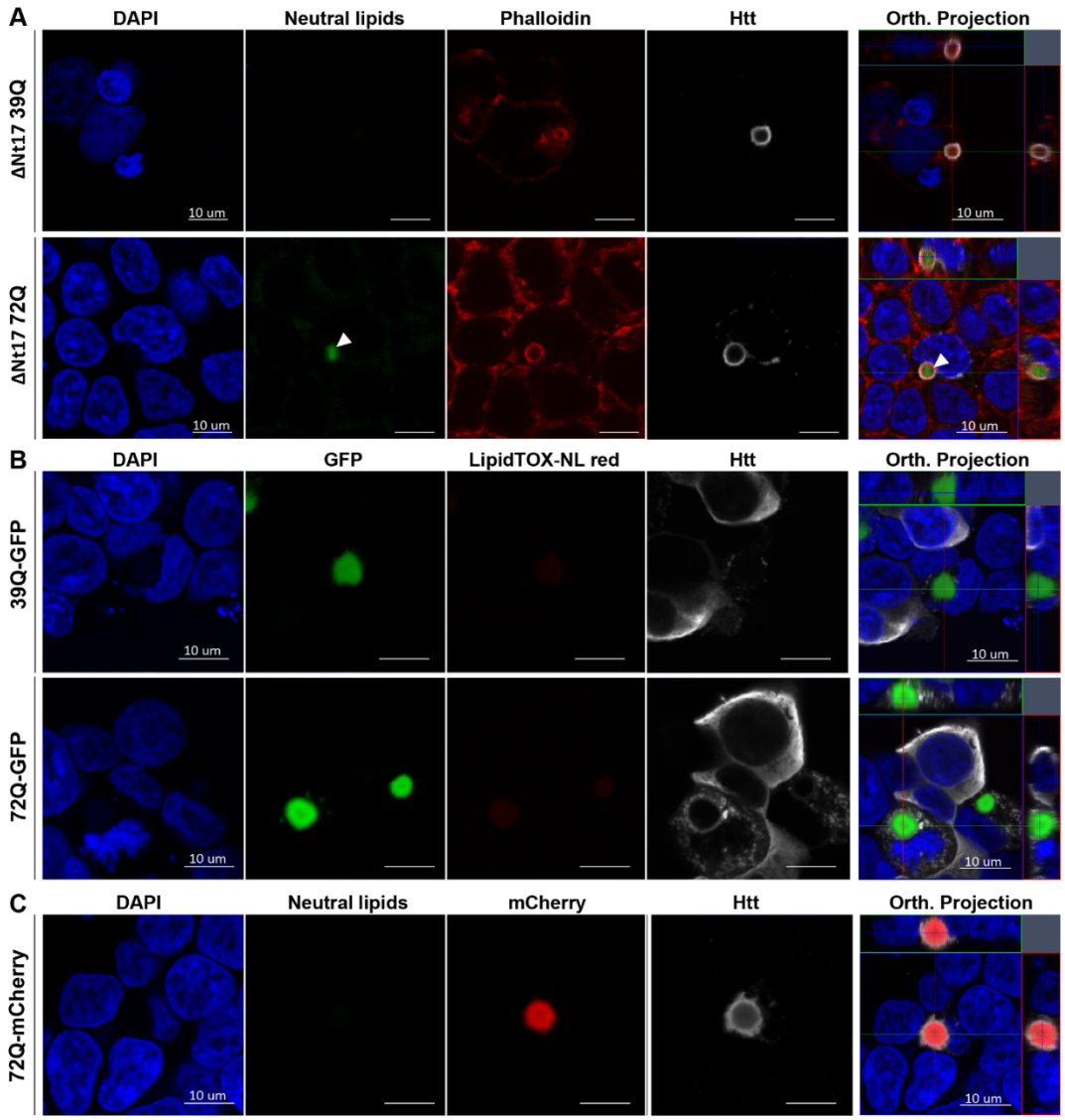

Figure S10. No neutral lipid enrichment was observed in Httex1-GFP cellular inclusions but only for Httex1 ΔNt17 72Q. A. Representative confocal image of Httex1 ΔNt17 39Q and 72Q inclusions 48h post-transfection stained with the non-Polar BODIPY probe (493/503) targeting neutral lipids (green) shows a neutral lipid enrichment to the core of the inclusion for 72Q but not 39Q. Phalloidin (red) was used to stain the F-actin. White arrowheads indicate neutral lipid enrichment. Scale bars = 10 µm. **B.** Representative confocal images of Httex1 39Q-GFP and Httex1 72Q-GFP inclusions 48h post-transfection stained with the LipidTOX™ Red stain targeting neutral lipids (LipidTOX-NL red). **C.** Representative confocal images of Httex1 72Q-mCherry inclusions 48h post-transfection stained with the non-Polar BODIPY probe (493/503) targeting neutral lipids. No lipid enrichment was observed for Httex1-GFP or Httex1-mCherry cellular inclusions. The nucleus was stained with DAPI (blue) and Httex1 with MAB5492 primary antibody revealed by a secondary antibody coupled to Alexa 647 (grey). Orthogonal projections (Orth. Projection) were generated from a Z-stack through the selected cells. Scale bars = 10 µm.

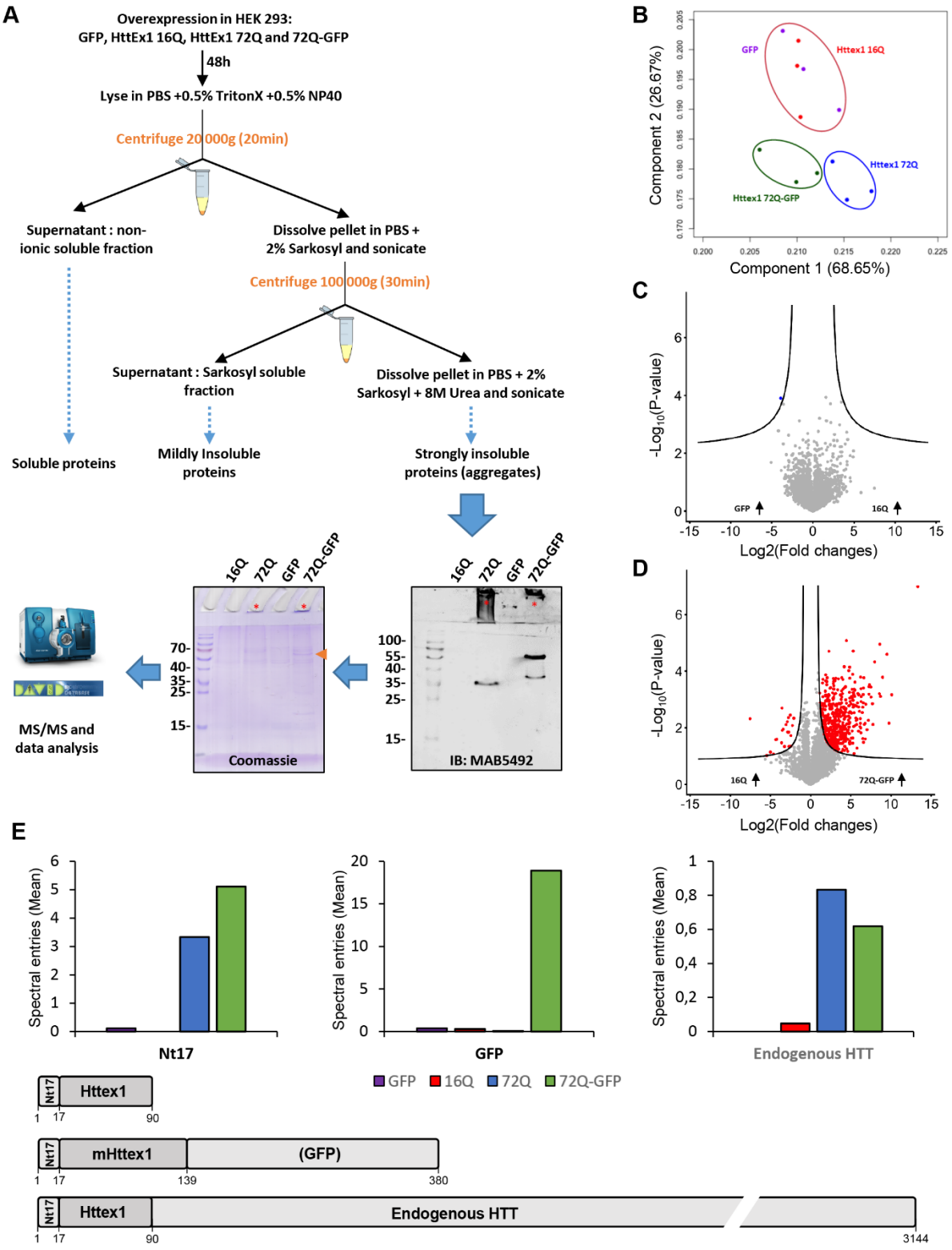

Figure S11. Detergent fractionation and proteomic analysis of Httex1 transfected in HEK cells. A. Overall workflow: HEK cells were transfected for 48h with Httex1 and GFP indicated plasmids before detergent fractionation from mild to harsh solubilization to separate soluble Htt to aggregate species. Proteins from the last Urea-insoluble fraction containing Htt inclusions were separated on SDS-PAGE gel, followed by LC-MS/MS for protein identification

and quantification of 3 independent experiments. Red stars indicate the presence of aggregates in the stacking gel. The orange arrow indicates the expected size of Httex1 72Q-GFP. **B.** Principal component analysis of the Urea-insoluble fraction shows 3 clusters: 1) Httex1 16Q and GFP (non-aggregated controls, red and purple), 2) Httex1 72Q-GFP (green), and 3) Httex1 72Q (blue). **C-D.** Volcano plot with a false discovery rate (FDR) of 0.05 and S0 of 0.5 used for the comparison of protein levels identified in the Urea-insoluble fraction. (**C**) Almost no significant differences were found in the comparison of the two negative controls Httex1 16Q and GFP. (**D**). The comparison of Httex1 72Q-GFP vs Httex1 16Q showed a strong protein enrichment for Httex1 72Q-GFP. **E.** Peptide detection (mean spectral entries of the 3 independent experiments) along the Httex1 (+/-GFP) and full-length HTT. The schematic representation of Htt fragments shows non-mutated Httex1 that corresponds to Httex1 16Q, mHttex1 corresponding to Httex1 72Q, or Httex1 72Q-GFP when fused to GFP at the C-terminus and the non-mutated full-length HTT that corresponds to the endogenous protein. The different sequences were divided into 4 segments: Nt17 domain, mHttex1 (not detected), GFP, and the full-length sequence of HTT over the first exon.

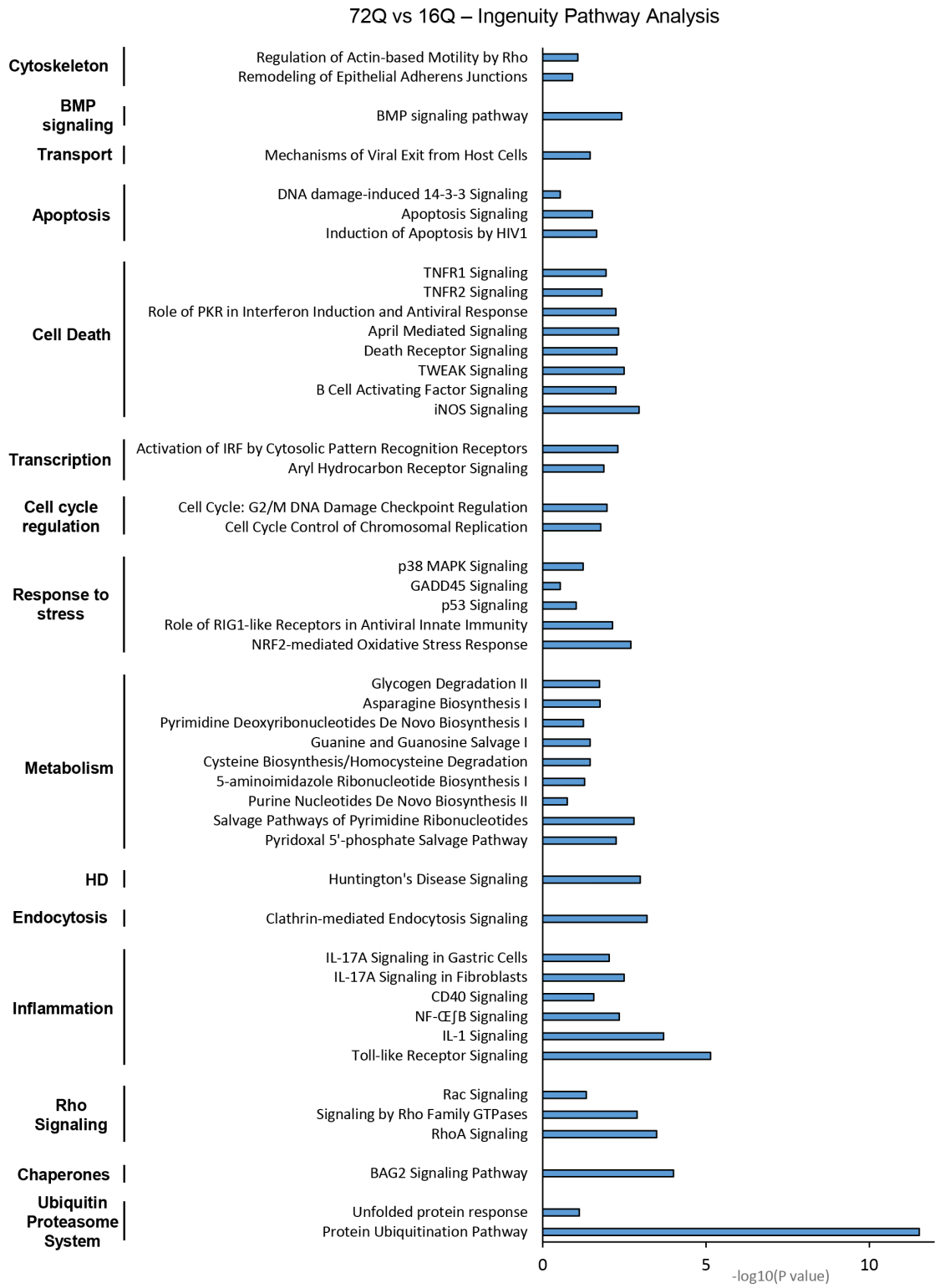

Figure S12. Ingenuity Pathway Analysis of Httex1 72Q vs Httex1 16Q Urea-insoluble fraction reveals strong enrichment of the Ubiquitin-Proteasome System (UPS). Canonical pathways enriched in the Urea-insoluble fraction of Httex1 72Q vs Httex1 16Q extracted from the volcano plot (Figure 3A) of the quantitative proteomic using Ingenuity Pathway Analysis (IPA).

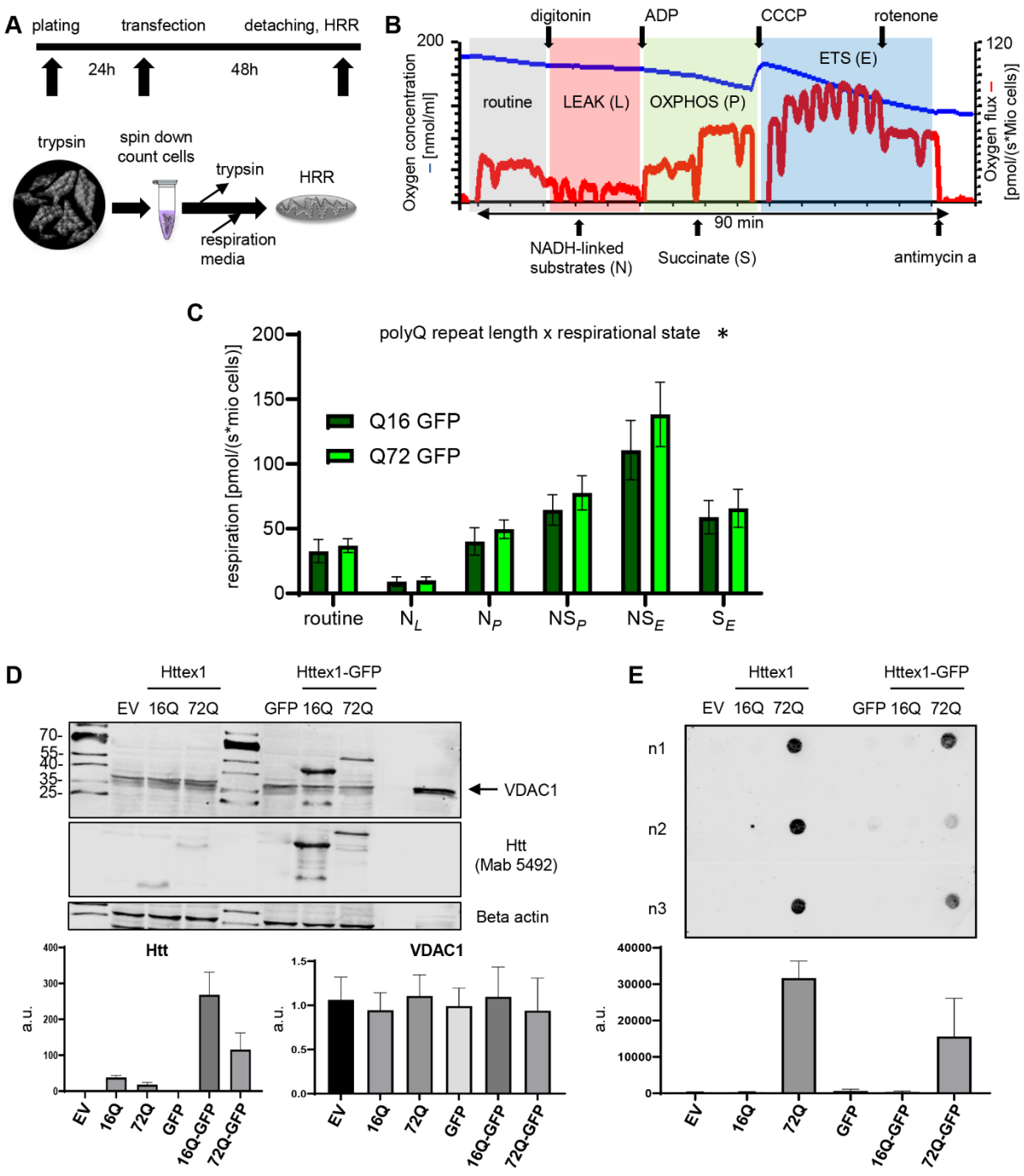

Figure S13. High-resolution respirometry (HRR) revealed respiration differences in cells transfected with Httex1 72Q-GFP compared to Httex1 16Q-GFP. A. Experimental setup of HRR experiments. Cells were transfected with indicated constructs 24h after plating in 4 independent experiments. Forty-eight hours after transfection, cells were gently detached and HRR was performed in respiration media (MIR05). **B.** After the measurement of routine respiration, cells were chemically permeabilized by digitonin. Different respirational states were subsequently induced using a substrate-uncoupler-inhibitor titration (SUIT) protocol. **C.** Routine respiration, NADH-driven, or complex 1-linked respiration after the addition of ADP

(OXPHOS state) (NP), NADH- and succinate driven, or complex 1 and 2-linked respiration in the OXPHOS state (NSP), and in the uncoupled electron transport system (ETS) capacity (NSE), as well as succinate driven, or complex 2-linked respiration in the ETS state (SE) were assessed. Httex1 72Q-GFP significantly increased the respiration compared to Httex1 16Q-GFP. **D.** Western Blot (WB) analyses of Httex1 transfected HEK cells in parallel with the HRR experiment. We quantified similar levels of the outer mitochondrial membrane protein VDAC1 indicating no decrease of mitochondrial density. Httex1 levels indicated higher levels of Httex1 16Q(+/-GFP) compared to Httex1 72Q(+/-GFP) in the soluble fraction. Due to better transfection efficiency, Httex1-GFP constructs are expressed higher than the tag-free Httex1 constructs. **E.** Filter trap (FT) analyses of Httex1 transfected HEK cells in parallel with the HRR experiment. Only Httex1 72Q(+/-GFP) were detected on the filter trap after loading of the SDS-insoluble fraction, indicating the formation of large SDS-insoluble aggregates. (C) ANOVA followed by Tukey honest significant difference [HSD] post hoc test was performed. *P < 0.05, **P < 0.005, ***P < 0.001.

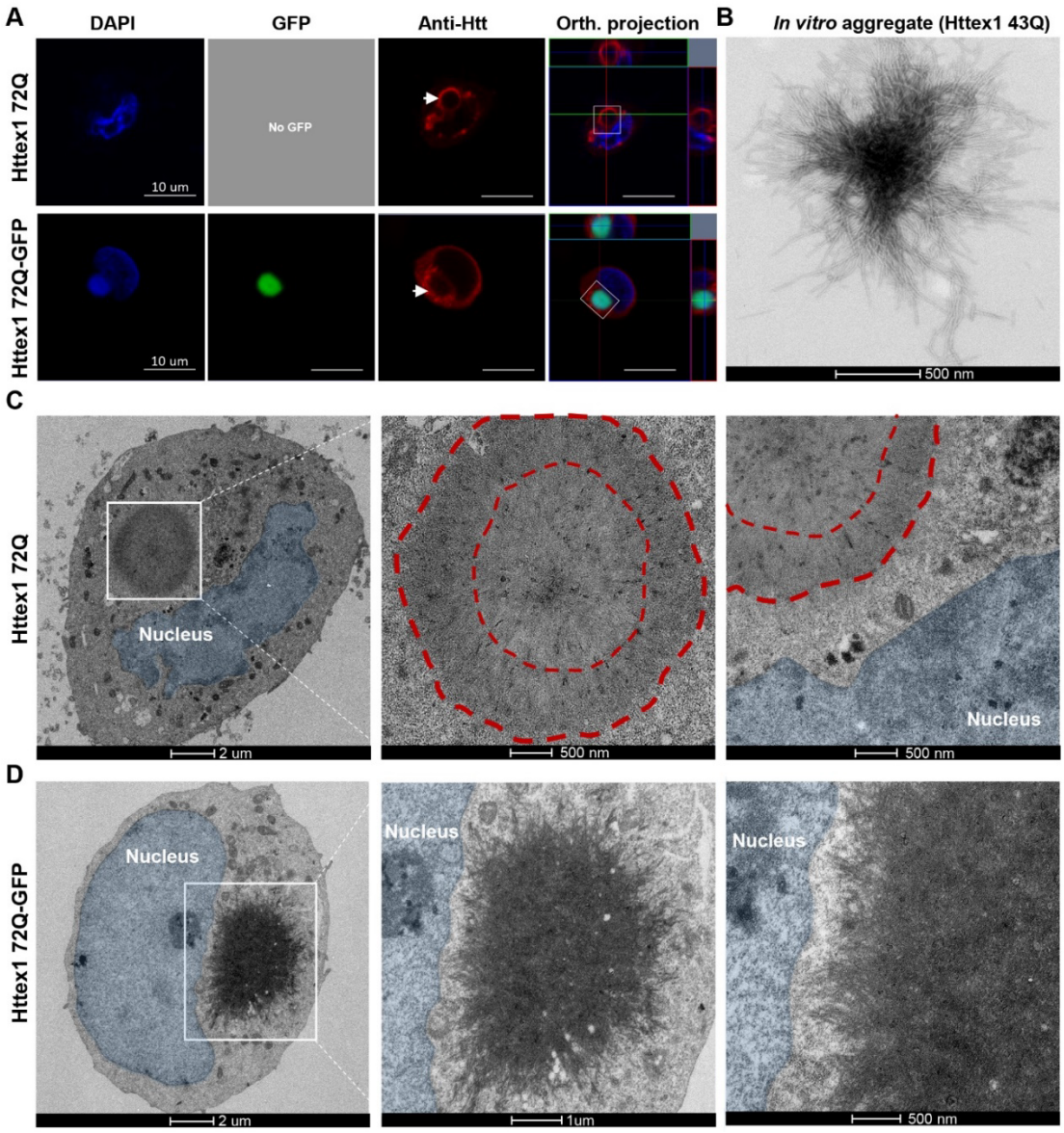

Figure S14. Correlative light- and electron microscopy (CLEM) of cells transfected with Httex1 72Q and Httex1 72Q-GFP. A. Confocal images of Httex1 72Q and Httex1 72Q-GFP, 48h after transfection in HEK cells. Httex1 expression (red) was detected using a specific primary antibody against the N-terminal part of Htt (MAB5492) or GFP (green), and the nucleus was stained with DAPI (blue). Scale bars = 10 µm. The same cell was then processed for EM. **B.** Representative image of *in vitro* aggregate of Httex1 43Q assessed by EM. **C.** Electron micrographs of the transfected cell by Httex1 72Q previously imaged by confocal (A, upper panels). Magnified micrographs of the inclusion (white square) and magnification close to the nuclear membrane are displayed on the middle and right-hand panels. **D.** Electron micrograph of the transfected cell by Httex1 72Q-GFP previously imaged by confocal (A, bottom panels). Magnified micrographs of the inclusion (white square) and magnification close to the nuclear membrane are displayed on the middle and right-hand panels. Scale bars = 2 µm, 1 µm, or 500nm as indicated below the micrographs.

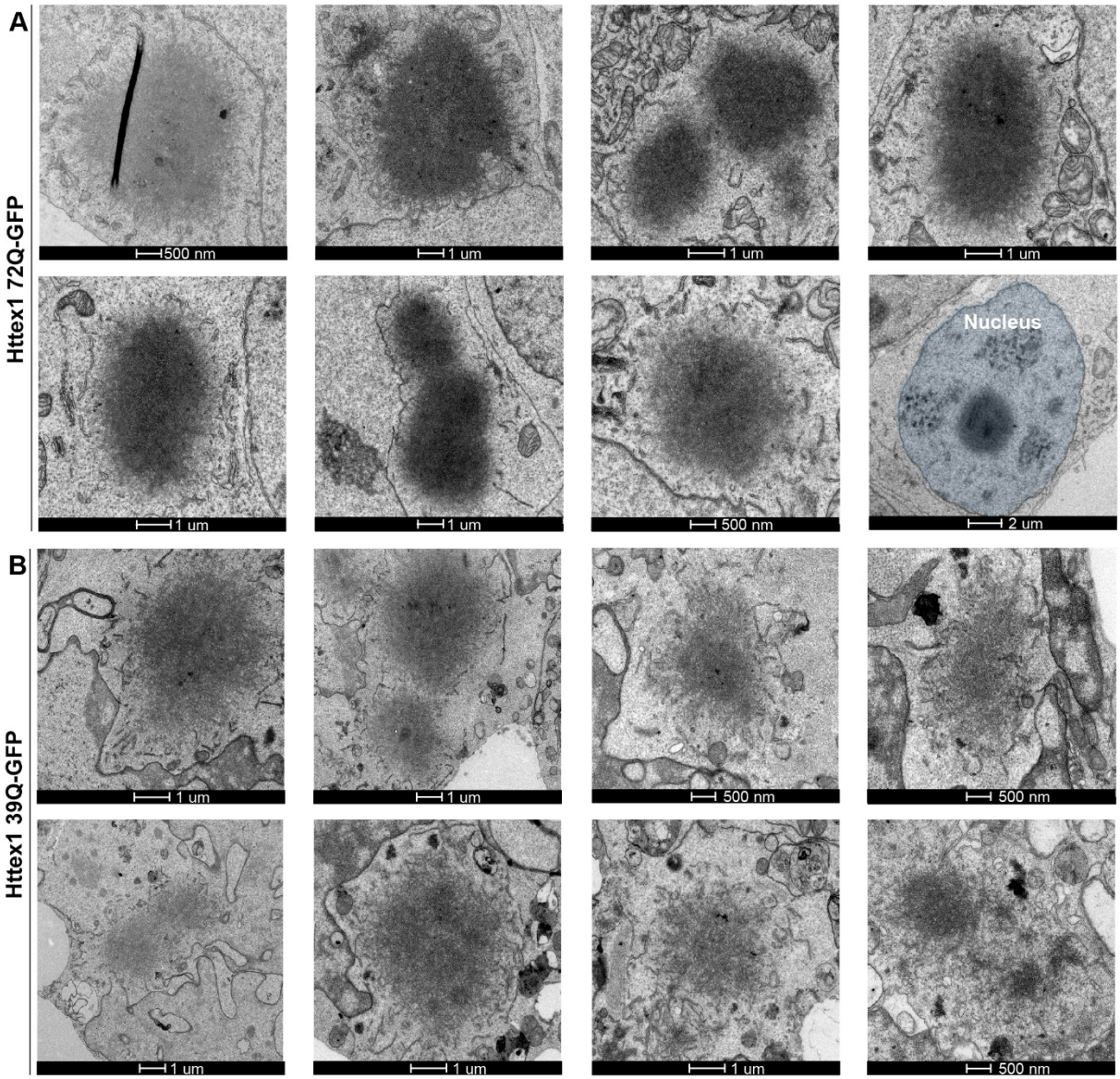

Figure S15. Ultrastructural characterization of Httex1 72Q-GFP and Httex1 39Q-GFP inclusions. A. 8 representative electron micrographs of Httex1 72Q-GFP inclusions in HEK cells 48h post-transfection. **B.** 8 representative electron micrographs of Httex1 39-GFP inclusions in HEK cells 48h post-transfection. The nucleus was highlighted in blue. Scale bar = 1 µm or 500 nm as indicated below the micrographs.

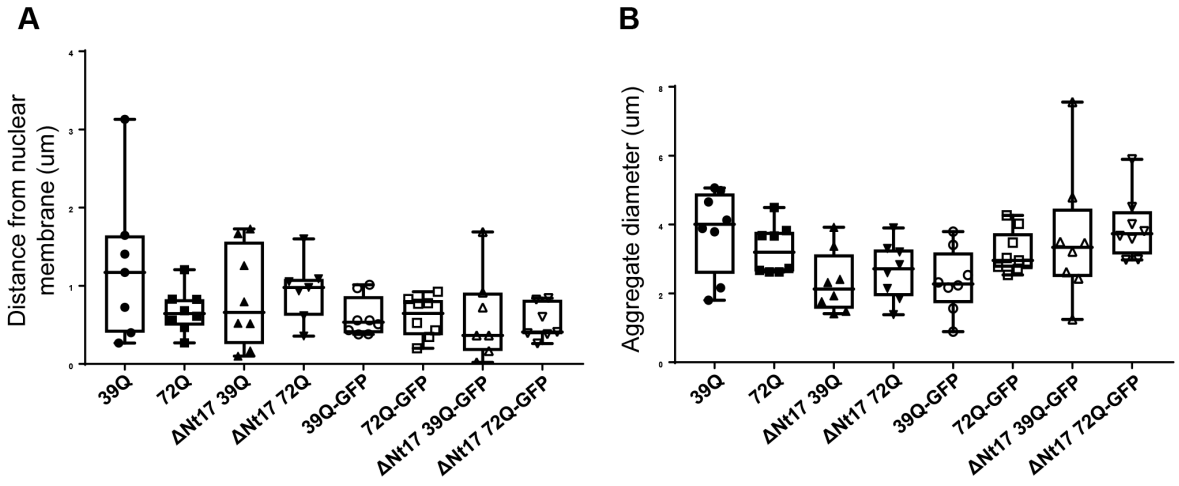

Figure S16. Subcellular localization and size of Httex1 inclusions based on electron micrographs. The distance of the inclusion from the nuclear membrane and the inclusion diameter was quantified from electron micrographs, Figures S3, S8, S15, and S18. **A.** Distance of the inclusion from the nuclear membrane. **B.** Httex1 inclusion diameter.

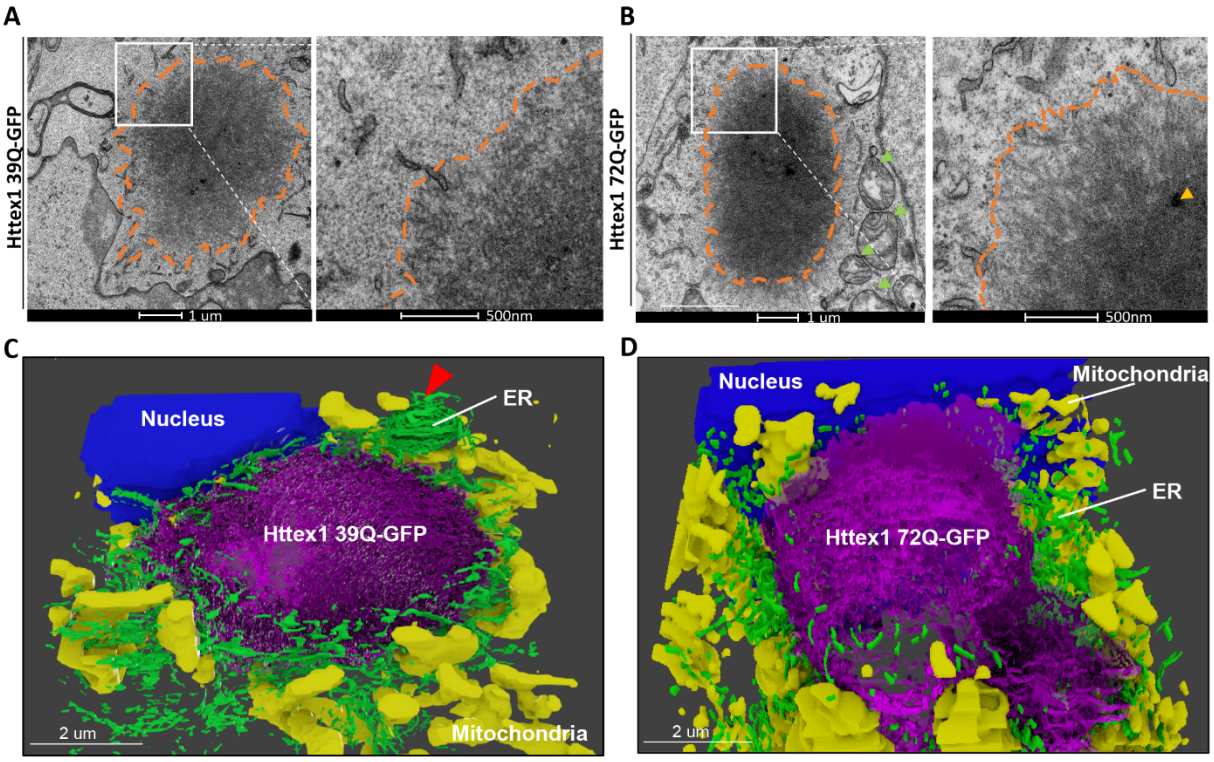

Figure S17. EM and 3D models of cellular Httex1 39Q-GFP and 72Q-GFP inclusions show ER and mitochondria in their periphery. A-B. Representative electron micrographs of Httex1 39Q-GFP (**A**) and Httex1 72Q-GFP (**B**) inclusions after 48h expression in HEK cells. Higher magnifications (white square) are represented in the right-hand panels. Dashed lines delimit the inclusions. Orange arrowheads: internalized membranous structures. Green arrowheads: mitochondria. More electron micrographs of Httex1 72Q-GFP (Figure S15A) and Httex1 39Q-GFP (Figure S15B) were acquired. Scale bars = 1 µm (left-hand panel) and 500 nm (right-hand panels). **C-D.** 3D models of Httex1 39Q-GFP (**C**) and Httex1 72Q-GFP (**D**) inclusions (top views). Httex1-GFP inclusions (purple), ER membranes (green), nucleus (blue), and mitochondria (yellow). Scale bars = 2 µm.

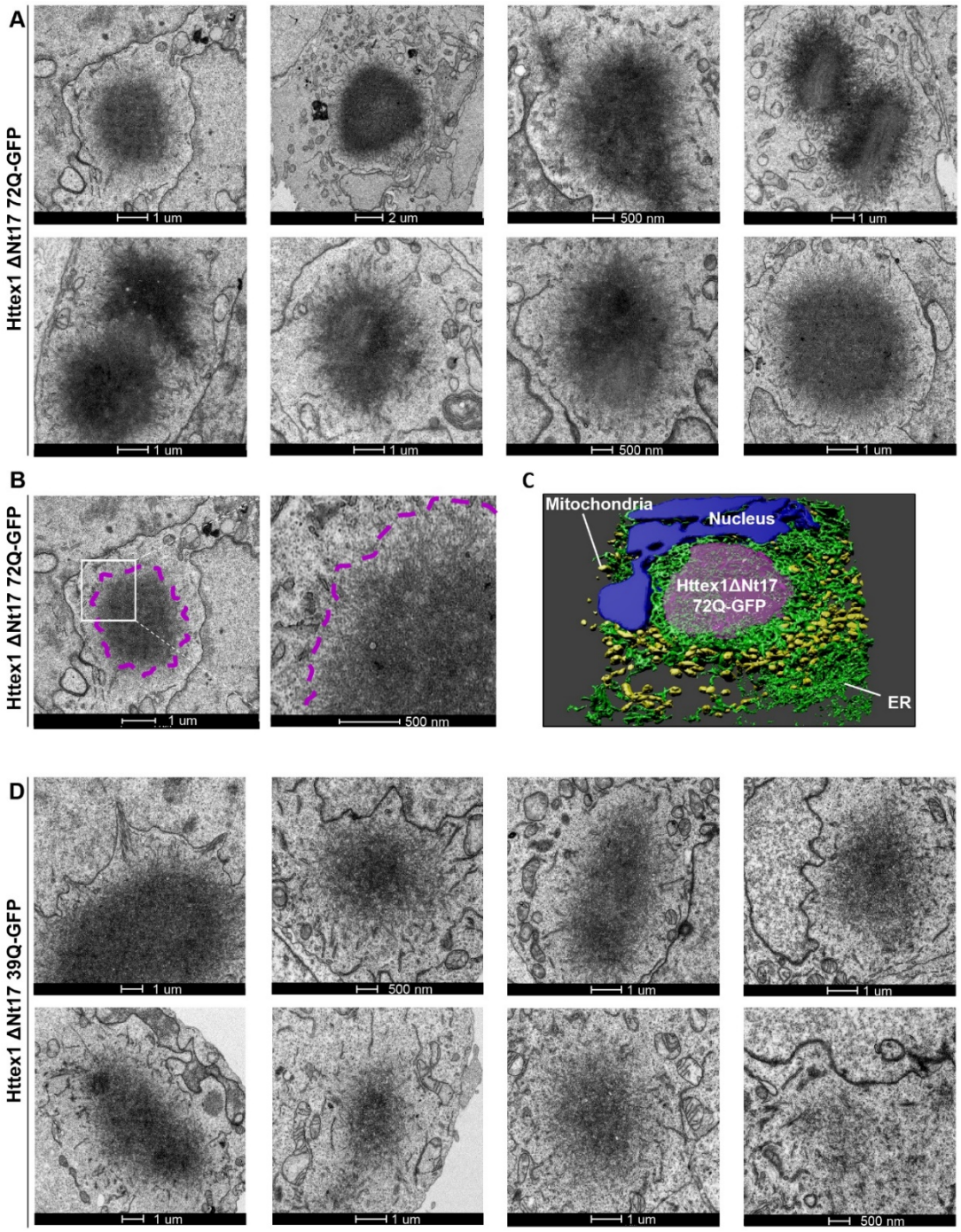

Figure S18. Ultrastructural characterization of Httex1 ΔNt17 72Q-GFP and Httex1 ΔNt17 39Q-GFP inclusions. A. 8 representative electron micrographs of Httex1 ΔNt17 72Q-GFP inclusions in HEK cells 48h post-transfection. **B.** Httex1 ΔNt17 72Q-GFP cellular inclusion and higher magnification (white square) displayed in the right-hand panel. Dashed lines delimit the inclusion. **C.** 3D model of Httex1 ΔNt17 72Q-GFP cellular inclusion (top view). Httex1 ΔNt17 72Q-GFP inclusion (purple), ER membranes (green), nucleus (blue), and mitochondria (yellow). **D.** 8 representative electron micrographs of Httex1 ΔNt17 39-GFP inclusions in HEK cells 48h post-transfection. Scale bar = 2 µm, 1 µm, or 500 nm as indicated below the micrographs.

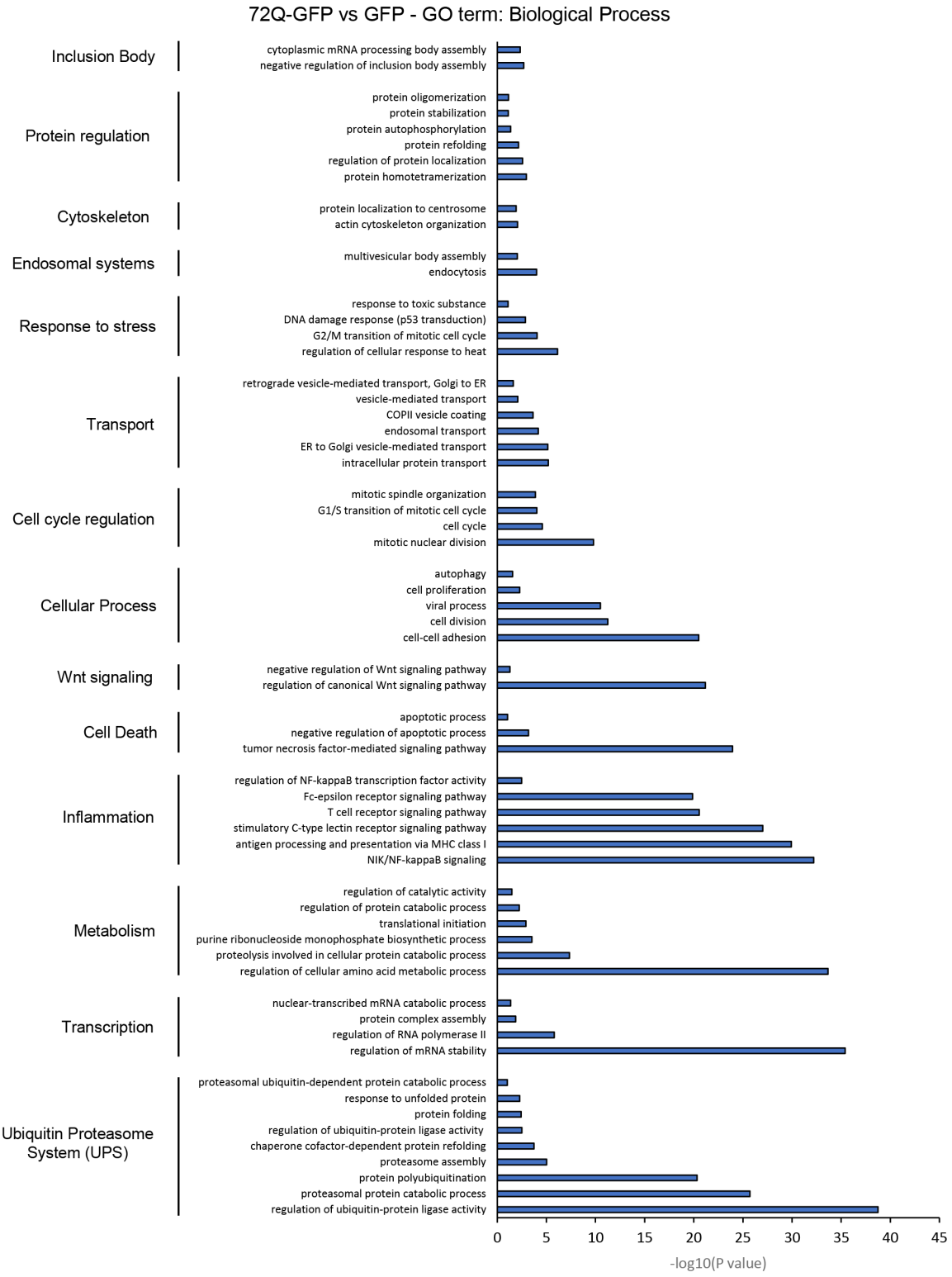

Figure S19. Gene Ontology (GO) analysis: Biological Process of Httex1 72Q-GFP vs GFP Urea-insoluble fraction. Classification of the proteins significantly enriched in the Urea-insoluble fractions of the HEK cells overexpressing Httex1 72Q-GFP versus GFP by biological processes using Gene Ontology (GO) enrichment analyses determined by DAVID analysis ($-\log_{10}$(p-value >1)).

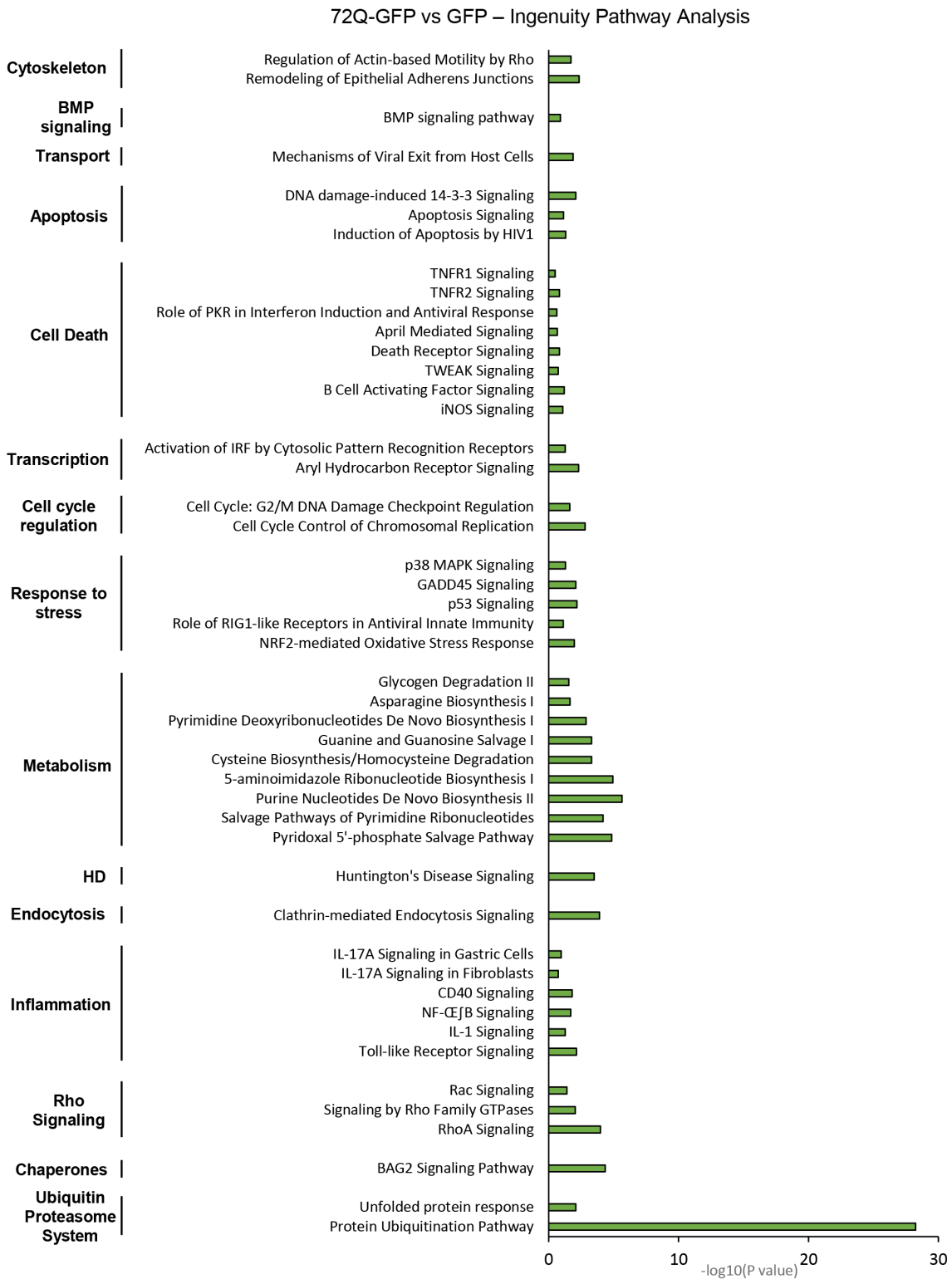

Figure S20. Ingenuity Pathway Analysis of Httex1 72Q-GFP vs GFP Urea-insoluble fraction. Canonical pathways enriched in the UREA-insoluble fraction of Httex1 72Q-GFP vs Httex1 GFP extracted from the volcano plot, Figure7A.

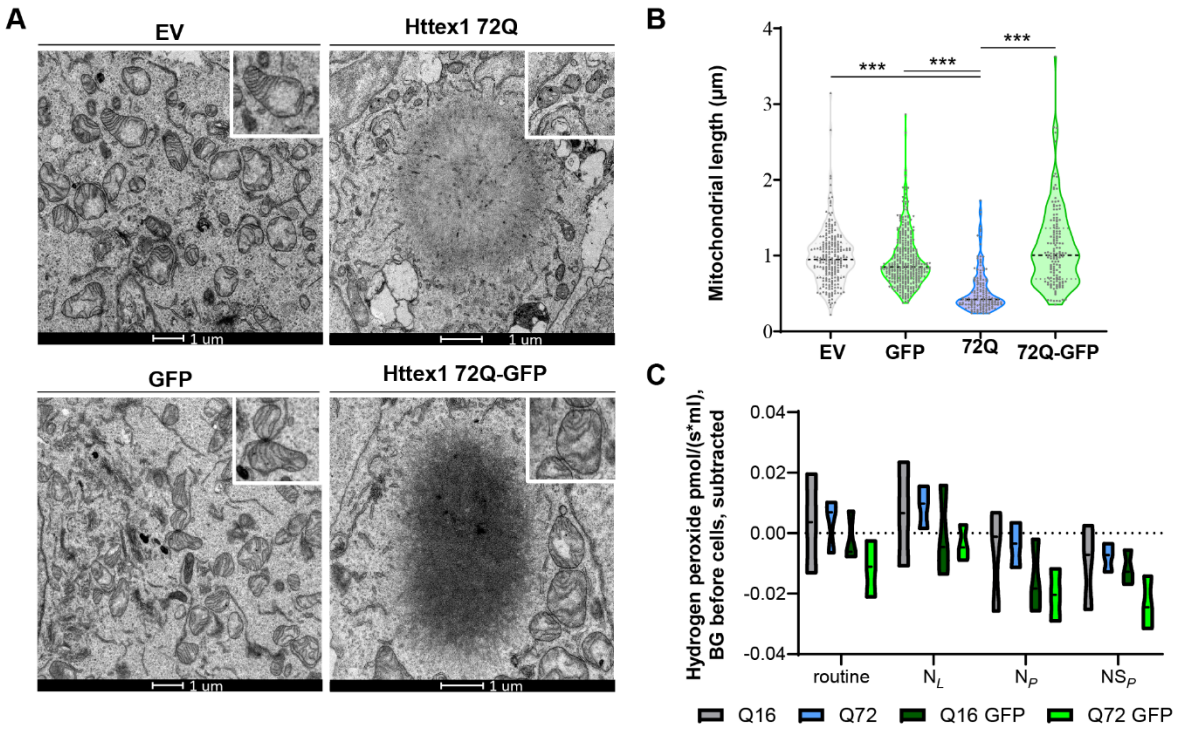

Figure S21. Formation of 72Q Httex1 inclusions induces mitochondrial alterations. A. Electron micrographs of mitochondria in HEK cells overexpressing EV (Empty Vector), Httex1 72Q, GFP or Httex1 72Q-GFP. The insets depict higher magnification of the mitochondria found at the periphery of Httex1 inclusions or representative in EV and GFP controls. Scale bars = 1 µm. **B.** Measurement of the mitochondrial length reveals a significant reduction of the size of the mitochondria profile located in the proximity of the inclusions. **C.** Mitochondrial reactive oxygen species (ROS) were measured in HEK cells overexpressing Httex1 16Q, Httex1 16Q-GFP, Httex1 72Q or Httex1 72Q-GFP for 48h. The most abundantly produced mitochondrial ROS were measured using Amplex red fluorometry (superoxide was transformed by superoxide dismutase to detectable levels of hydrogen peroxide). No significant differences of mitochondrial ROS levels were detected in the HEK cells overexpressing Httex1 72Q, compared to Httex1 72Q-GFP. The graph presents the median, minimum and maximum values of three independent experiments. ANOVA followed by Tukey honest significant difference [HSD] post hoc test was performed. *P < 0.05, **P < 0.005, ***P < 0.001.

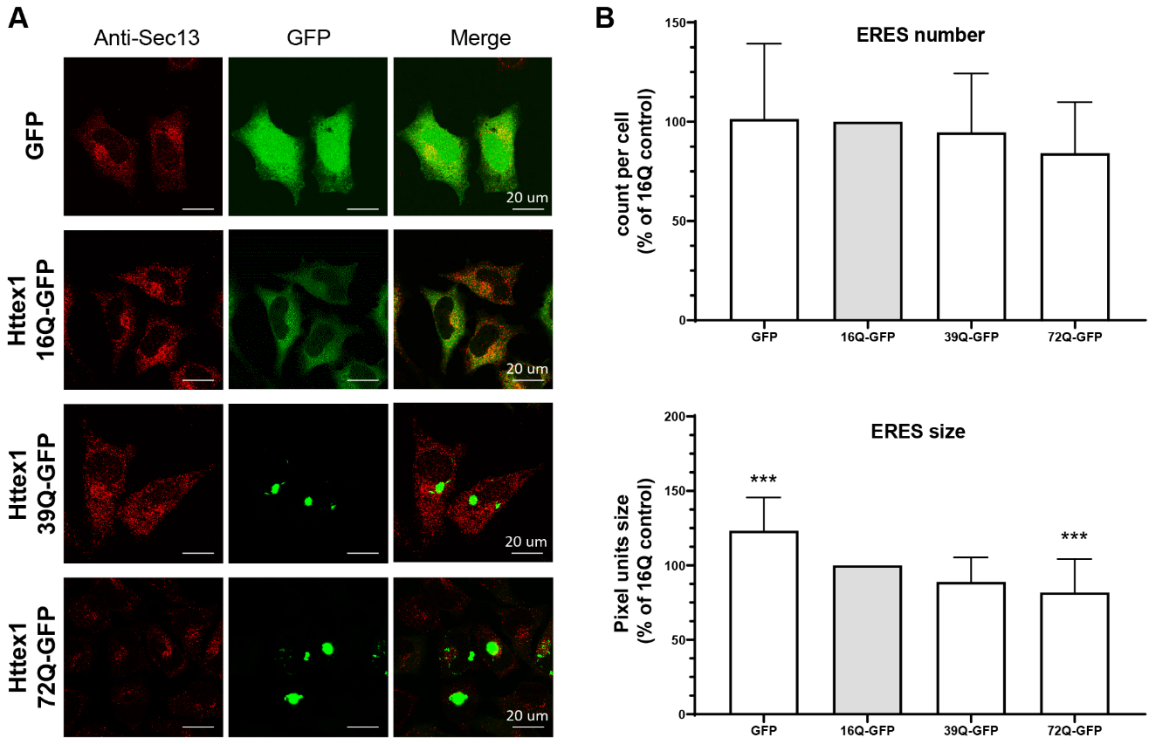

Figure S22. Httex1-GFP inclusion formation induces the size reduction of ER-exit sites. **A.** Representative confocal images of HeLa cells transfected with Httex1 16Q-GFP, 39Q-GFP or 72Q-GFP or GFP (as the negative control). Cells were fixed 48h after transfection and immunostained. Httex1-GFP or GFP was detected by fluorescence and ER exit sites were detected using the Sec13 antibody (red). Scale bars = 20 μm. **B**. ERES number and size quantification from confocal imaging was performed using FIJI. The graphs represent the mean ± SD of three independent experiments, which are presented as the relative percentage of the Httex1 16Q-GFP control. ANOVA followed by Tukey honest significant difference [HSD] post hoc test was performed. *P < 0.05, **P < 0.005, ***P < 0.001.

Specific features	Httex1 72Q	Httex1 72Q-GFP
Actin F at the periphery of inclusions	+++	-
Ring detection of Htt Ab.	+++	++ (+center faintly)
Core/shell organization	+++	-
Thickness and spacing of fibrils in periphery	Thin fibrils and more spacing than the core	Thick fibrils, more inter-space compare to tag-free
polyQ influence on ultrastructure	Yes (lose core/shell organization)	No
Recruitment of membranous organelles	++ in core and +++ in periphery	Few but interactions at the periphery
Nuclear inclusions	Lose core/shell arrangement and the recruitment of membranous organelles No interactions with nuc. mb.	No overall change in morphology No interactions with nuc. mb.
Lipids	++ Neutral lipids in core specific for 72Q not 39Q	-
Mitochondrial morphology	Loss of cristae	normal
Fragmentation of mitochondrial profile	++	-
Mitochondrial respiration	++	+
ER impact	++ ERES modulation	+ ERES modulation
Main pathways proteomic	Endolysosome, UPS, cytoskeleton, nucleoplasm, ER to Golgi transport	Endolysosome, UPS, cytoskeleton, nucleoplasm, ER to Golgi transport, mitochondria
Differences in proteomic pathways	Infection/inflammation, mRNA stability	UPS more enriched, mitochondria, metabolism

Figure S23. Tag-free and GFP Httex1 cellular inclusions reveal distinct features.

The table summarizes the key distinct features between Httex1 72Q and Httex1 72Q-GFP at cellular, ultrastructural, proteomic composition and functional levels. Confocal analysis revealed a ring-like detection of Httex1 by Htt antibodies and the colocalization with filamentous actin only for tag-free Httex1. We identified the core and shell structural organization of tag-free Httex1, influenced by the subcellular environment, as well as the polyQ length but not the Nt17 domain. Cellular Httex1 inclusions are structurally different from GFP-tagged Httex1 in term of fibrillar arrangement and inter-spacing. Additionally, no core and shell organization was detected for Httex1-GFP, independent of the polyQ length. We demonstrated that neutral lipids are specifically recruited in tag-free Httex1 72Q inclusions. Tag-free and GFP Httex1 inclusions also impacted (differentially) the cellular organelles with a pronounced fragmentation and loss of cristae for mitochondria in close proximity to Httex1 72Q inclusions. Therefore, tag-free Httex1 72Q transfected cells were found to have a larger increase in mitochondrial respiration and ER trafficking modulation. Finally, our quantitative proteomic analysis revealed 55% differences between the co-aggregated proteins with Httex1 compared to Httex1-GFP. Httex1 72Q inclusions were found to have a specific enrichment of infection and inflammation related proteins, while Httex1 72Q-GFP exhibited a stronger UPS-related protein enrichment, as well as an enrichment of mitochondria and metabolic-related pathways.